Proteinuric chronic kidney disease is associated with altered red blood cell lifespan, deformability and metabolism

OPEN

Rosi Bissinger[1], Travis Nemkov[2], Angelo D'Alessandro[2,3], Marijke Grau[4], Thomas Dietz[4], Bernhard N. Bohnert[1,5,6], Daniel Essigke[1], Matthias Wörn[1], Lina Schaefer[1], Mengyun Xiao[1], Jonathan M. Beirne[2], M. Zaher Kalo[1], Anja Schork[1,5,6], Tamam Bakchoul[7], Kingsley Omage[1], Lingsi Kong[1], Irene Gonzalez-Menendez[8], Leticia Quintanilla-Martinez[8], Birgit Fehrenbacher[9], Martin Schaller[9], Achal Dhariwal[10], Andreas L. Birkenfeld[1,5,6], Florian Grahammer[11], Syed M. Qadri[12] and Ferruh Artunc[1,5,6]

[1]Division of Endocrinology, Diabetology and Nephrology, Department of Internal Medicine, University Hospital Tübingen, Tübingen, Germany; [2]Department of Biochemistry and Molecular Genetics, University of Colorado Anschutz Medical Campus, Aurora, Colorado, USA; [3]Division of Hematology, University of Colorado Denver, Aurora, Colorado, USA; [4]Institute of Molecular and Cellular Sports Medicine, German Sport University of Cologne, Köln, Germany; [5]Institute of Diabetes Research and Metabolic Diseases (IDM) of the Helmholtz Center Munich at the University Tübingen, Tübingen, Germany; [6]German Center for Diabetes Research (DZD) at the University Tübingen, Tübingen, Germany; [7]Center for Clinical Transfusion Medicine, University Hospital of Tübingen, Tübingen, Germany; [8]Department of Pathology, University of Tübingen, Tübingen, Germany; [9]Department of Dermatology, Eberhard Karls University Tübingen, Tübingen, Germany; [10]Institute of Oral Biology, Faculty of Dentistry, University of Oslo, Oslo, Norway; [11]Department of Medicine, University Medical Center Hamburg-Eppendorf, Hamburg, Germany; and [12]Faculty of Health Sciences, Ontario Tech University, Oshawa, Ontario, Canada

Anemia is a common complication of chronic kidney disease, affecting the quality of life of patients. Among various factors, such as iron and erythropoietin deficiency, reduced red blood cell (RBC) lifespan has been implicated in the pathogenesis of anemia. However, mechanistic data on *in vivo* RBC dysfunction in kidney disease are lacking. Herein, we describe the development of chronic kidney disease-associated anemia in mice with proteinuric kidney disease resulting from either administration of doxorubicin or an inducible podocin deficiency. In both experimental models, anemia manifested at day 10 and progressed at day 30 despite increased circulating erythropoietin levels and erythropoiesis in the bone marrow and spleen. Circulating RBCs in both mouse models displayed altered morphology and diminished osmotic-sensitive deformability together with increased phosphatidylserine externalization on the outer plasma membrane, a hallmark of RBC death. Fluorescence-labelling of RBCs at day 20 of mice with doxorubicin-induced kidney disease revealed premature clearance from the circulation. Metabolomic analyses of RBCs from both mouse models demonstrated temporal changes in redox recycling pathways and Lands' cycle, a membrane lipid remodeling process. Anemic patients with proteinuric kidney disease had an increased proportion of circulating phosphatidylserine-positive RBCs. Thus, our observations suggest that reduced RBC lifespan, mediated by altered RBC metabolism, reduced RBC deformability, and enhanced cell death contribute to the development of anemia in proteinuric kidney disease.

Kidney International (2021) ■, ■–■; https://doi.org/10.1016/j.kint.2021.08.024

KEYWORDS: anemia; cell death; deformability; kidney disease; Lands' cycle; metabolism; proteinuria; red blood cells; redox recycling

Translational Statement

This study demonstrates that proteinuric kidney disease in murine models leads to premature red blood cell (RBC) clearance, ultimately causing the development of anemia. Increased RBC death also occurs in patients with chronic kidney disease and anemia. RBC dysfunction in the uremic milieu is an important mechanism for RBC loss and the development of renal anemia, irrespective of endogenous erythropoietin secretion.

The development of anemia is a typical complication of advanced chronic kidney disease (CKD) and is associated with impaired quality of life,[1] increased risk for cardiovascular events[2] and hospitalization,[3] and cognitive decline.[4] The severity of anemia has been viewed as an independent predictor of mortality in both dialysis- and non–dialysis-dependent CKD patients.[5] The pathophysiology of renal anemia is complex and involves iron and erythropoietin (EPO) deficiency in the setting of low-grade inflammation, which, in turn, compromise normal erythropoiesis in CKD

Correspondence: *Ferruh Artunc, Division of Endocrinology, Diabetology and Nephrology, Department of Internal Medicine, University Hospital Tuebingen, Otfried-Mueller-Strasse 10, 72076 Tuebingen, Germany. E-mail: ferruh.artunc@med.uni-tuebingen.de*

Received 3 March 2021; revised 5 August 2021; accepted 13 August 2021

patients.[6] In advanced CKD, the EPO response is inadequately low in relation to the degree of anemia.[7,8] The high prevalence of concomitant iron deficiency in CKD is a consequence of disturbed iron homeostasis.[9] A neglected mechanism of iron loss in CKD is proteinuria, which can lead to urinary losses of transferrin-bound iron (up to 0.3 mg/d) when proteinuria reaches the nephrotic range.[10]

Another factor that is thought to contribute to renal anemia in CKD patients is the shortened lifespan of red blood cells (RBCs), first described >60 years ago.[6,11,12] A recent study using a carbon monoxide breath test demonstrated that the RBC lifespan progressively decreased from 120 days in patients with stage 1 CKD to 60 days in patients with stage 5 CKD.[13] Notably, transfusion of allogenic RBCs from healthy donors to CKD patients was followed by a rapid clearance of transfused RBCs without evidence of hemolysis.[12] A plausible mechanism for this observation may be the stimulation of apoptosis-like cell death in anucleate RBCs, denoting an injury pattern in which the cell membrane integrity is not compromised and the cytoplasmic content remains intact.[14] RBCs undergoing cell death exhibit various morphologic alterations resulting from cytoskeletal damage, such as surface bleb formation, loss of membrane elasticity, and/or cellular dehydration.[15] On a molecular level, RBC death is associated with intracellular Ca^{2+} accumulation, altered cellular energy status, and breakdown of phospholipid asymmetry, ultimately leading to externalization of phosphatidylserine (PS) on the outer plasma membrane.[15,16] As a consequence, macrophages and specialized dendritic cells swiftly recognize PS-externalized RBCs, leading to erythrophagocytosis and their catabolism in spleen and liver.[17]

Because of the confounding pathophysiology of renal anemia in humans, animal studies are warranted to pinpoint the contributing mechanisms. Doxorubicin-induced nephropathy (DIN) in 129S1/SvImJ mice[18] and mice with inducible podocin deficiency (*Nphs2*$^{\Delta ipod}$)[19] are 2 models that are characterized by the induction of nephrotic-range proteinuria within days, progression to renal failure after 3 weeks, and death in 6 to 7 weeks.[19–21] Both mouse models effectively recapitulate all stages of human CKD. In the present study, we tested whether progressive renal failure in these mice with proteinuric kidney disease affects RBC lifespan and contributes to anemia. In parallel, we examined RBC phenotype in blood drawn from CKD patients with nephrotic-range proteinuria.

METHODS

Detailed information about the materials and methods is provided in the supplementary file.

Mouse studies

Experiments were performed on 8-week-old wild-type 129S1/SvImJ mice of both sexes (Charles River). DIN was induced by a single injection of doxorubicin (14.5 μg/g body weight), as described previously.[18] To control for the myelotoxic effect of doxorubicin unrelated to the development of nephropathy, doxorubicin-resistant C57BL/6 mice were also subjected to the same treatment protocol.[22]

In addition, similar experiments were conducted on 8-week-old mice with inducible deletion of podocin (B6-*Nphs2*$^{tm3.1Antc}$*Tg[*Nphs1*-rtTA*3G]^{8Jhm}*Tg[tetO-cre]^{1Jaw}) or *Nphs2*$^{\Delta ipod}$ mice, which were treated with doxycycline for 14 days.[19] All animal experiments were conducted according to the National Institutes of Health *Guide for the Care and Use of Laboratory Animals* and the German Law for the Welfare of Animals, with approval from the local authorities (Regierungspräsidium Tübingen, approval numbers M12/17 and M17/19G).

The experimental design of the mouse studies is outlined in Supplementary Figure S1.

Patients

The patient study was conducted in compliance with the Declaration of Helsinki and was approved by the local ethics committee of the University Hospital Tübingen (556/2018BO2). Lithium-heparin blood and urine samples were obtained from patients with nephrotic-range proteinuria and preserved glomerular filtration rate (GFR; stages 1–2; n = 10) and patients with reduced GFR (CKD stage 3–5; n = 15) at the University Hospital Tübingen. As a control group, blood from age- and sex-matched healthy volunteers (n = 25) was provided by the blood bank of the University Hospital Tübingen. All human samples were collected after informed consent. Clinical characteristics of the patients are stated in Table 1.

Flow cytometry analyses

Different parameters of RBC cell death were determined by flow cytometry.[14] To determine RBC lifespan *in vivo*, 25 μl of 5(6)-CFDA, SE dye was injected at a concentration of 9.96 mM (solubilized in dimethylsulfoxide) into the retro-orbital plexus of wild-type 129S1/SvImJ and doxorubicin-injected mice, as described previously.[23] At the indicated time points, blood was drawn from the retro-orbital plexus of the mice, and the percentage of 5(6)-CFDA, SE^+ cells was detected by flow cytometry analysis. Finally, data were analyzed using FlowJo software (FlowJo LLC).

RBC deformability and osmotic gradient ektacytometry

RBC deformability was measured using the Laser-Assisted Optical Rotational Cell Analyzer (LORCA MaxSis; RR Mechatronics), which has been described in detail elsewhere.[24] The osmotic gradient ektacytometry (osmoscan) analyses were also performed using the LORCA MaxSis and measure deformability under various osmotic conditions.[25]

Histologic examination

For hematoxylin and eosin staining, spleens and femurs were stained with hematoxylin and eosin. All slides were stained with the primary antibody Ter119 (BD Pharmingen; dilution 1:500). For periodic acid–Schiff staining, 2.5-μm-thick slices of the kidneys were stained with periodic acid–Schiff reagent (Carl Roth) and hematoxylin (abcam). May-Grünwald-Giemsa staining (Pappenheim method) was performed to determine RBC shape changes, as described previously.[26] Glomeruli isolation was done by using a biotinylation approach and cell sorting.[19] For protein detection of podocin, an antibody from Sigma was applied (P0372).[19] Roti-Mount Fluor Care DAPI (Carl Roth) was used to stain nuclei.

Ultra-high-performance liquid chromatography–mass spectrometry metabolomics from mouse RBCs

Analyses were performed as previously published.[27] Briefly, the analytical platform employs a Vanquish ultra-high-performance

Table 1 | Characteristics of the CKD patients and healthy blood donors

Parameter	CKD due to primary nephrotic syndrome with preserved GFR (>60 ml/min per 1.73 m^2)	Proteinuric CKD with reduced GFR (<60 ml/min per 1.73 m^2)	Healthy blood donors
No. and gender of patients	10 (3♀, 7♂)	15 (7♀, 8♂)	25 (10♀, 15♂)
Age, yr	44 (32–62)	63 (52–75)	59 (46–63)
Cause of nephrotic syndrome/CKD			
Focal segmental glomerulonephritis	1	2	
Minimal change glomerulopathy	3		
Membranous glomerulonephritis	6	1	
Focal segmental glomerular sclerosis			
Interstitial nephritis		2	
Diabetic nephropathy		6	
ANCA-positive vasculitis		1	
Polycystic kidney disease		1	
AL-amyloidosis		1	
Unknown		1	
Plasma creatinine concentration, mg/dl	1.0 (0.8–1)	2.2 (1.5–3.3)[a]	0.7 (0.7–0.9)
GFR-CKD-EPI, ml/min per 1.73 m^2	90 (69–90)	31 (16–49)[a]	
Plasma urea, mg/dl	36 (26–48)	90 (62–141)[b]	
Plasma total protein, g/dl	5.5 (4.5–6.6)	6.5 (6–6.9)	
Plasma C-reactive protein, mg/dl	0.03 (0.01–0.29)	0.37 (0.09–0.96)	0.04 (0.01–0.17)
Proteinuria, mg/g creatinine	6362 (4467–8141)	3624 (676–7681)	
MCV, fl	87 (85–88)	85 (80–90)[c]	90 (87–93)
MCHC, g/dl	34.9 (34.3–35.5)[c]	34.3 (33–35.6)	32.8 (32.5–33.8)
Hematocrit, %	41.9 (39.1–44.7)	35.2 (32–37.1)[a]	43.5 (41.6–45)
Concurrent medication			
Diuretics	7	12	
RAS blocker	9	12	
Immunosuppressants	5	6	
Anticoagulants	3	3	
Statins	6	9	
Proton-pump inhibitors	3	7	
Vitamin D	6	8	
Phosphate binders		2	
ESA		2	
Bicarbonate		6	

AL, xxx; ANCA, anti–neutrophil cytoplasmic antibody; CKD, chronic kidney disease; EPI, Epidemiology Collaboration; ESA, xxx; GFR, glomerular filtration rate; MCHC, mean corpuscular hemoglobin concentration; MCV, mean corpuscular volume; RAS, renin-angiotensin system.
Values are given as number or median (interquartile range).

liquid chromatography system (Thermo Fisher Scientific) coupled online to a Q Exactive mass spectrometer (Thermo Fisher Scientific).

Statistical analyses

Data are provided as arithmetic means ± SEM or as median with interquartile range (25th–75th percentile) with *n* representing the number of used animals or included patients, respectively. Data were tested for normality with the Kolmogorov-Smirnov test, the D'Agostino test, and the Shapiro-Wilk test. Variances were analyzed by Bartlett test for equal variances. Tukey or Dunn multiple-comparison posttest, unpaired Student *t* test, or Mann-Whitney *U* test was performed by GraphPad Prism 8 (GraphPad Software). $P < 0.05$ with 2-tailed testing was considered statistically significant. Additional graphs were plotted through GraphPad Prism 8.

RESULTS

Experimental proteinuric kidney disease induces anemia in mice

After induction, 129S1/SvImJ mice with DIN and *Nphs2*$^{\Delta ipod}$ mice developed nephrotic-range proteinuria (Figure 1a and Supplementary Figure S2C) and progressive renal failure characterized by high plasma urea levels from day 20 onwards (Figure 1b and Supplementary Figure S2D). During the first 10 days, mice experienced body weight gain with ascites (Figure 1c and Supplementary Figure S2E), reflecting sodium retention caused by the excretion of serine proteases or proteasuria.[18] After spontaneous reversal of sodium retention, these mice steadily lost weight. In mice with DIN and in *Nphs2*$^{\Delta ipod}$ mice, light microscopy images, captured after 10 days, revealed typical histomorphologic changes consistent with focal segmental glomerular sclerosis (Figure 1d and Supplementary Figure S2B). These were absent in doxorubicin-injected C57BL/6 mice (Figure 1d). Doxorubicin treatment induced a strong decline in hemoglobin, RBC count, and hematocrit (Figure 1e–g) from day 10 on in 129S1/SvImJ and C57BL/6 mice, which in the latter were normalized at days 20 and 30. In contrast, on days 20 and 30, doxorubicin-injected 129S1/SvImJ and podocin-deficient mice developed progressive anemia, characterized by reduced mean corpuscular volume (Figure 1h) and reduced hemoglobin (Supplementary Figure S2F), suggesting that

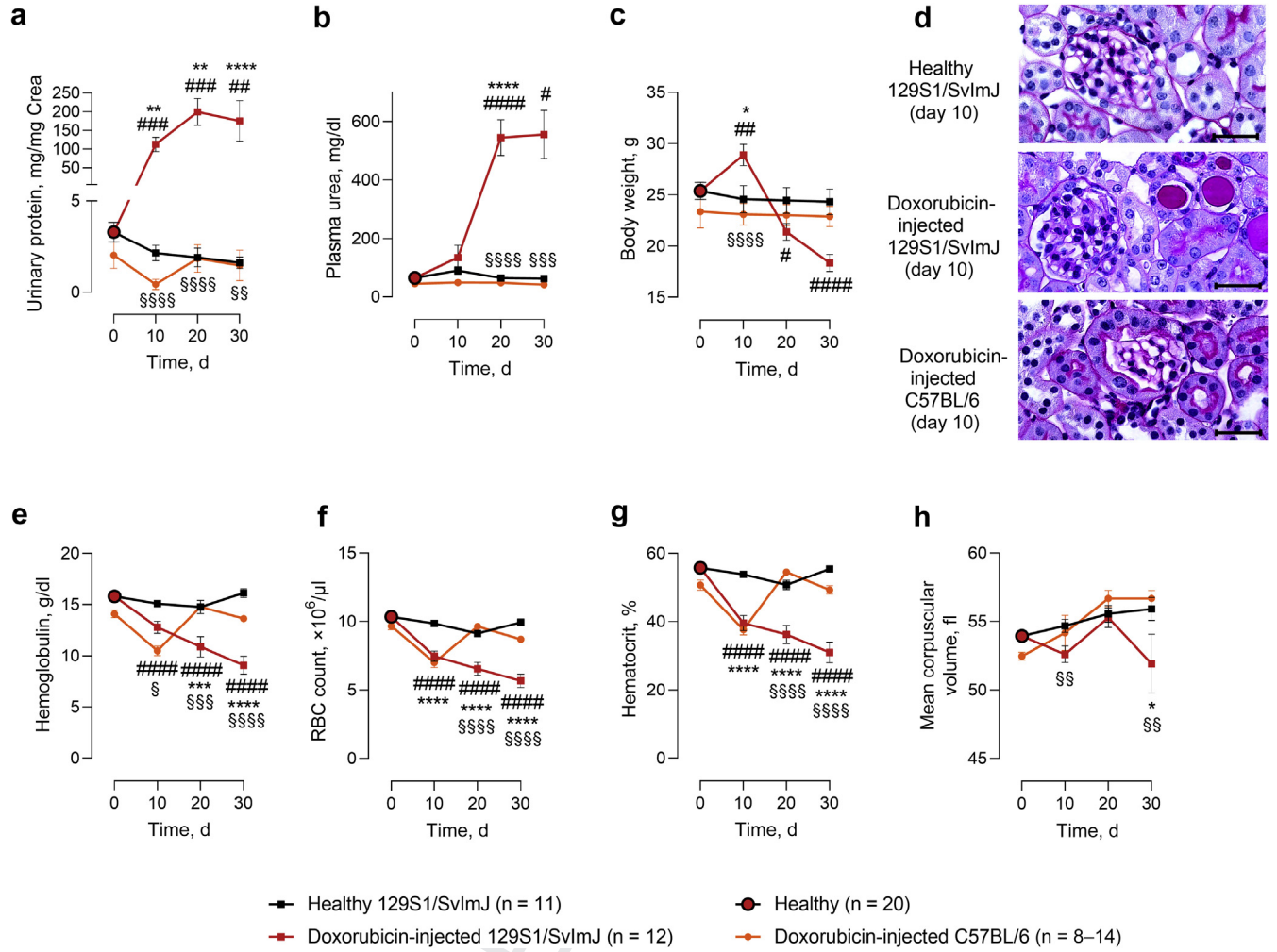

Figure 1 | Renal function and overt anemia in doxorubicin-injected 129S1/SvImJ mice. (**a**–**d**) Doxorubicin-injected 129S1/SvImJ mice developed (**a**) high proteinuria, (**b**) progressive increase of plasma urea concentration, (**c**) transient body weight increase, and (**d**) typical histomorphologic changes indicative of focal segmental glomerular sclerosis on day 10 (periodic acid–Schiff staining; bar = 10 µm). (**e**–**h**) In addition, these mice developed anemia reflected by (**e**) a decreased hemoglobin level, (**f**) lower red blood cell (RBC) numbers, (**g**) diminished hematocrit levels, and (**h**) decreased mean corpuscular volume. (**a**–**d**) Doxorubicin-injected C57BL/6 mice did not show any sign of kidney injury, and (**e**–**g**) anemia on day 10 was normalized on days 20 and 30. Arithmetic means ± SEM are shown. *Significant difference between healthy 129S1/SvImJ and doxorubicin-injected 129S1/SvImJ mice; #significant difference to baseline of doxorubicin-injected 129S1/SvImJ mice; §significant difference between doxorubicin-injected 129S1/SvImJ and doxorubicin-injected C57BL/6 mice. To optimize viewing of this image, please see the online version of this article at www.kidney-international.org. Crea, creatinine.

anemia is associated with progressive renal failure and not with doxorubicin treatment *per se*.

Anemia in experimental proteinuric kidney disease is not caused by compromised erythropoiesis

Both anemic mouse models displayed a significant increase in the percentage of circulating reticulocytes (Figure 2a and Supplementary Figure S3C). Plasma EPO concentrations were dramatically increased at day 10 in 129S1/SvImJ with DIN and healthy C57BL/6 mice but were normalized again on days 20 and 30 (Figure 2b). In podocin-deficient mice, plasma EPO concentrations spiked at day 10 and remained increased at days 20 and 30 (Supplementary Figure S2H). In histologic analyses from bone marrow and spleen, the number of erythroid precursor cells compared with myeloid precursors was increased at day 30 (Figure 2d–g), pointing to stimulated erythropoiesis in anemic 129S1/SvImJ mice with DIN.

Reduced RBC lifespan is the primary cause of anemia in experimental proteinuric kidney disease

Externalization of PS on the outer leaflet of the RBC plasma membrane is an indicator of cell death and a promoter of erythrophagocytosis.[14] RBC cell death was quantified using fluorescence-activated cell sorting analyses of fluorescent annexin V–bound surface PS.[14] In freshly drawn blood, the percentage of PS-exposing cells was >4-fold higher on day 20 in mice with DIN (4.16% ± 0.86%) compared with healthy mice (1.00% ± 0.11%) (Figure 3a). Similarly, *Nphs2*$^{\Delta ipod}$ mice showed an approximate 2-fold increase in PS exposure (1.27% ± 0.20%) compared with healthy mice (0.58% ±

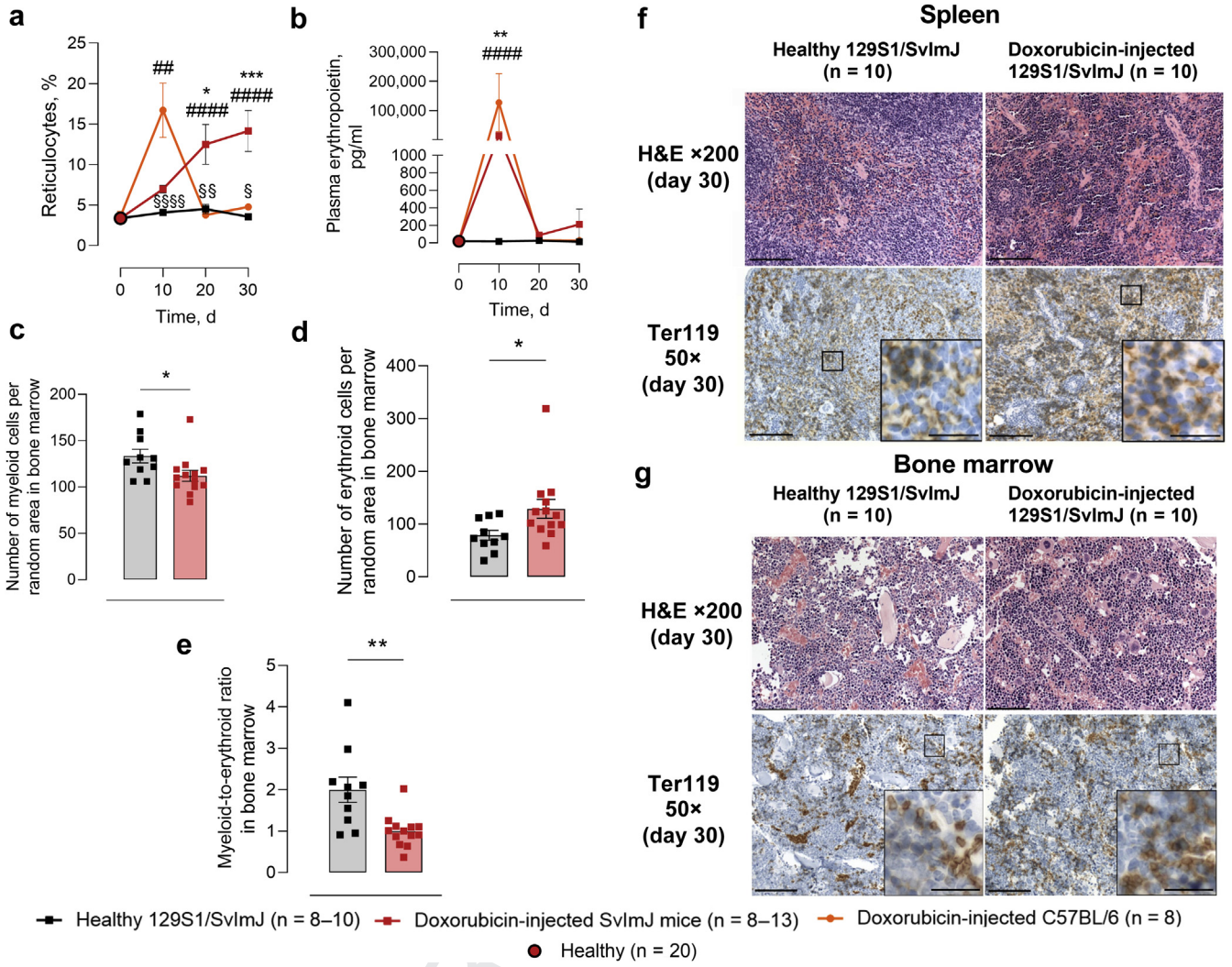

Figure 2 | Erythropoiesis is stimulated in doxorubicin-injected 129S1/SvImJ mice with anemia. (**a**) Anemia in doxorubicin-injected 129S1/SvImJ mice occurred despite increased reticulocyte numbers at days 20 and 30. (**b**) Plasma erythropoietin concentration was highly increased at day 10 in doxorubicin-injected 129S1/SvImJ and C57BL/6 mice, but was normalized again on days 20 and 30. (**c**–**e**) Quantification of the absolute numbers of (**c**) myeloid and (**d**) erythroid cells in bone marrow, and the (**e**) ratio of myeloid-to-erythroid cells in healthy and doxorubicin-injected 129S1/SvImJ mice in bone marrow showed a higher number of erythroid precursor cells in doxorubicin-injected 129S1/SvImJ mice on day 30. (**f,g**) The (**f**) spleen and (**g**) bone marrow histology showed an increase in erythroid precursor cells, observed even at lower magnification, in doxorubicin-injected 129S1/SvImJ mice (right panels) compared with healthy mice (left panels) on day 30. (**f,g**) Ter119 immunohistochemistry (lower panels) supported the hematoxylin and eosin (H&E) findings. Ter119 is positive in the erythroid precursors (nucleated cells) and in the red blood cells (nonnucleated cells). Bar = 100 μm; insets = 25 μm. Arithmetic means ± SEM are shown. *Significant difference between healthy 129S1/SvImJ and doxorubicin-injected 129S1/SvImJ mice; #significant difference to baseline of doxorubicin-injected 129S1/SvImJ mice; §significant difference between doxorubicin-injected 129S1/SvImJ and doxorubicin-injected C57BL/6 mice. To optimize viewing of this image, please see the online version of this article at www.kidney-international.org.

0.05%) on day 30 (Supplementary Figure S3A). It is known that RBCs are eliminated from the circulation by macrophages residing in the spleen.[17] This observation may, therefore, explain the higher spleen/body weight ratio of *Nphs2*$^{\Delta ipod}$ mice (Supplementary Figure S2G), wherein twice as many RBCs are degraded compared with healthy C57BL/6 mice.

As nephrotic-range proteinuria leads to dysproteinemia,[28] we further investigated whether enhanced RBC cell death may be stimulated by a component in the plasma of mice with DIN. As depicted in Figure 3b, PS exposure at days 10 and 20 was twice as high following incubation (30 minutes at 37 °C) of healthy RBCs in plasma of doxorubicin-injected 129S1/SvImJ mice compared with incubation in plasma of healthy mice. Ca^{2+} influx into RBCs, mediated by voltage-gated and voltage-independent nonselective cation channels,[29,30] is one of the key regulators of RBC cell death. In RBCs collected at days 20 and 30 from 129S1/SvImJ mice with DIN, intracellular Ca^{2+} concentrations were increased (Figure 3c); this phenomenon was recapitulated in *Nphs2*$^{\Delta ipod}$ mice on day 20 (Supplementary Figure S3B).

In both mouse models, there was a significant negative correlation of the percentage of PS-positive RBCs, with

FLA 5.6.0 DTD ■ KINT2759_proof ■ 7 October 2021 ■ 12:12 am ■ ce

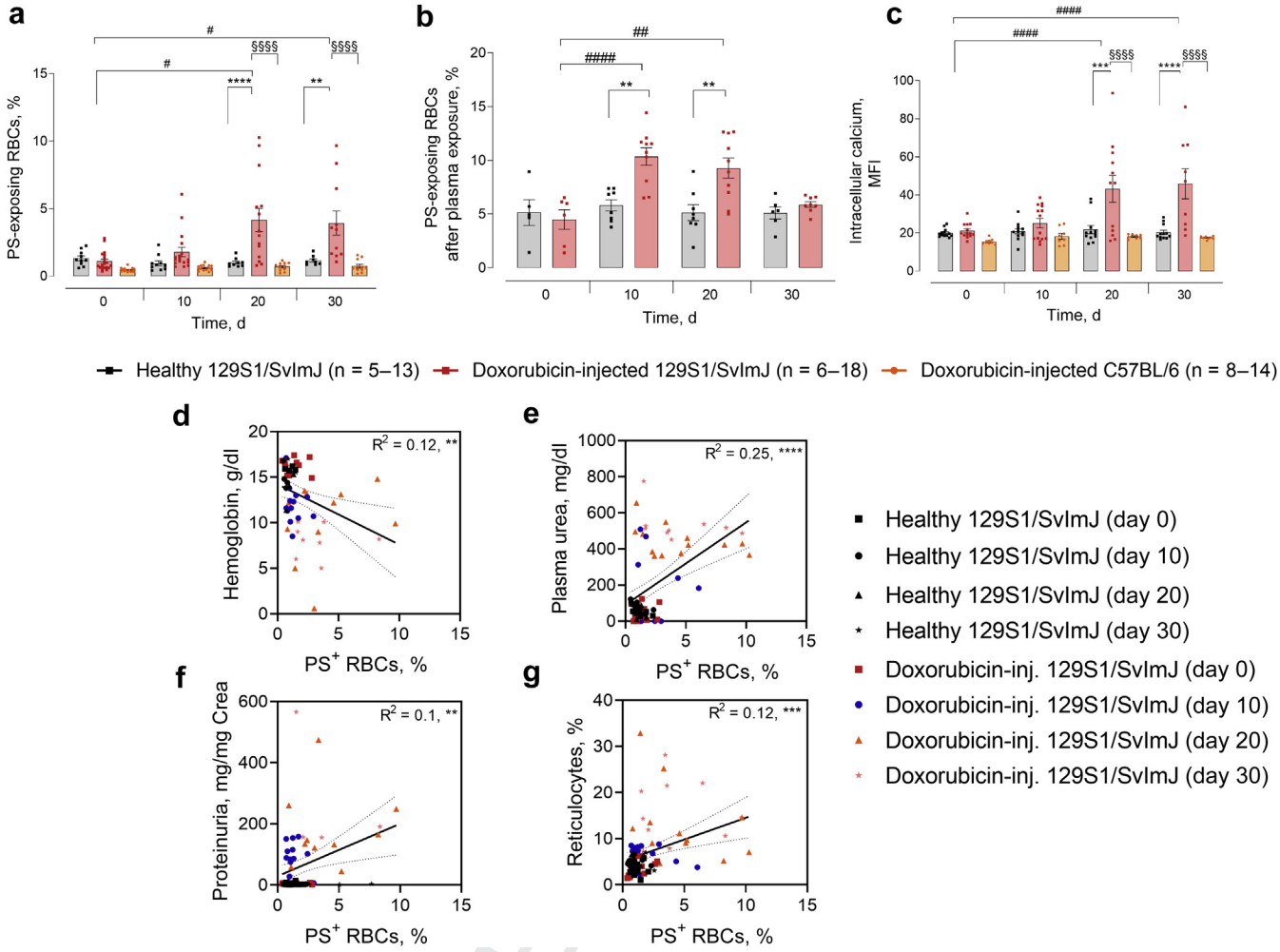

Figure 3 | Mice with doxorubicin-induced nephropathy develop enhanced red blood cell (RBC) death mediated by increased intracellular calcium levels. (**a**) Externalization of phosphatidylserine (PS), reflecting RBC death, was enhanced on days 20 and 30 after induction of doxorubicin-induced nephropathy. (**b**) Incubation of healthy RBCs in plasma taken on days 10 and 20 from these mice led to PS externalization. (**c**) PS externalization was accompanied by enhanced intracellular calcium levels of RBCs taken on days 20 and 30 after induction. (**d**–**g**) The (**d**) percentage of PS-exposing RBCs was correlated with hemoglobin levels, and kidney damage was indicated by (**e**) plasma urea concentration and (**f**) proteinuria, as well as with (**g**) reticulocyte formation. (**d**–**g**) Data include each time point (0, 10, 20 and 30 days) of each healthy 129S1/SvImJ and 129S1/SvImJ mouse with doxorubicin-induced nephropathy. Arithmetic means ± SEM are shown. *Significant difference between healthy 129S1/SvImJ and doxorubicin-injected (inj.) 129S1/SvImJ mice; #significant difference to baseline of doxorubicin-injected 129S1/SvImJ mice; §significant difference between doxorubicin-injected 129S1/SvImJ and doxorubicin-injected C57BL/6 mice. Crea, creatinine; MFI, mean fluorescence intensity.

severity of anemia reflected by hemoglobin levels (Figure 3d and Supplementary Figure S3D). Moreover, there was a significant correlation with kidney damage reflected by plasma urea concentration (Figure 3e and Supplementary Figure S3E) and to a lesser degree with proteinuria (Figure 3f and Supplementary Figure S3F). To compensate RBC loss in anemia, formation of new RBCs was stimulated in both mice, as indicated by increased percentage of circulating reticulocytes, and was significantly correlated with the magnitude of PS-exposing RBCs (Figure 3g and Supplementary Figure S3G).

Doxorubicin-induced renal injury alters murine RBC lifespan, morphology, and biophysical properties

Twenty days after induction of DIN, coinciding with the development of reduced renal function (Figure 1b), the fluorescent dye 5(6)-CFDA, SE,[23] which is rapidly taken up into RBCs, was i.v. injected to examine RBC clearance rate at the indicated time points *in vivo*. Representative histograms, shown in Figure 4a, indicate the removal of labeled RBCs from the circulation and replacement by unlabeled RBCs. Increased RBC loss was already apparent 3 days after administration of the dye, and clearance of RBCs was significantly faster in 129S1/SvImJ mice with DIN up to day 37. On day 41, ≈17% more RBCs were removed from the circulation in these mice compared with healthy mice (Figure 4b).

Images taken from a blood smear revealed morphologic changes in RBCs drawn from 129S1/SvImJ mice with DIN (Figure 4c) and *Nphs2*$^{\Delta ipod}$ mice (Supplementary Figure S4A). In healthy mice, RBCs display a biconcave disc

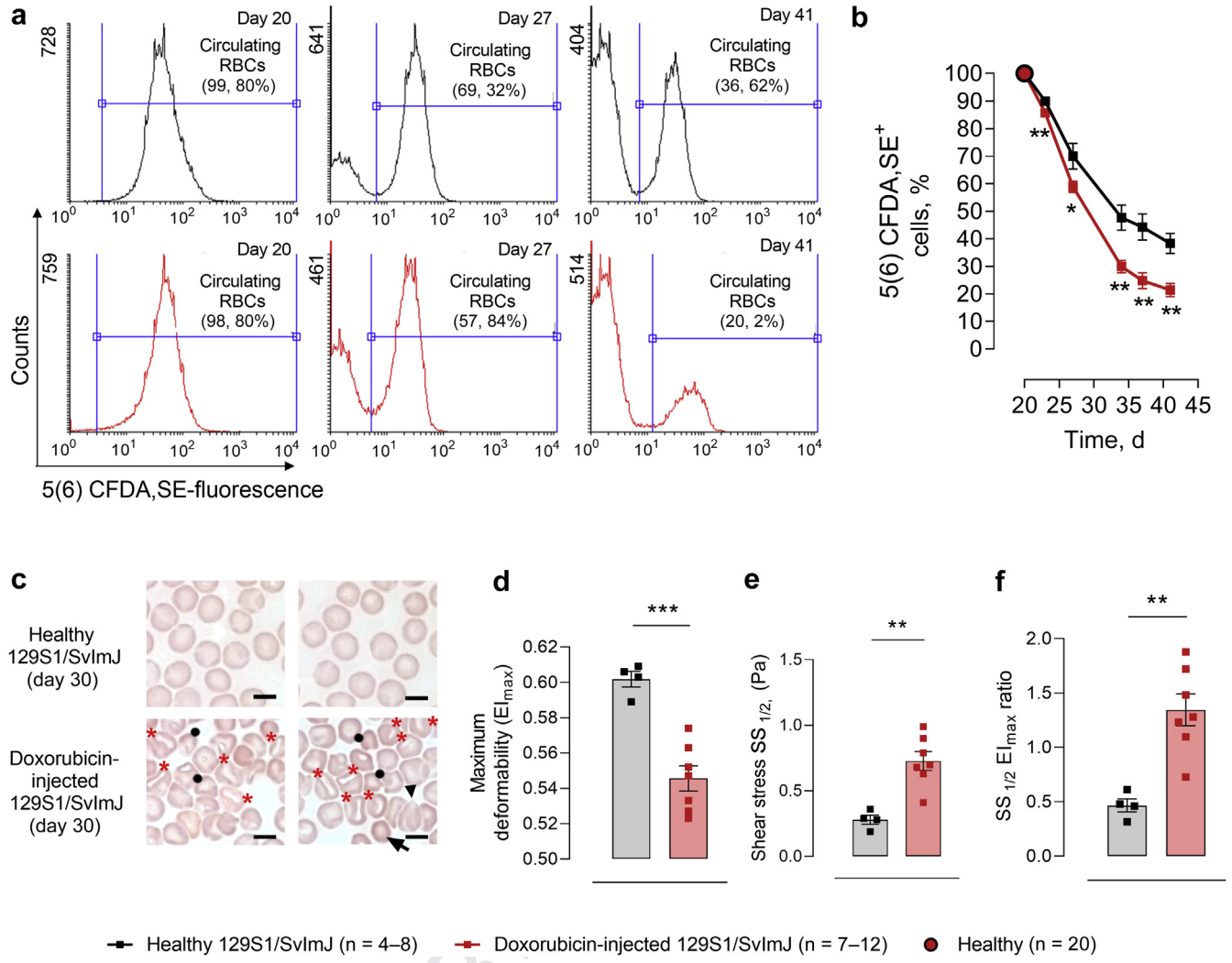

Figure 4| Shortened red blood cell (RBC) survival and altered morphology of RBCs in in mice with doxorubicin-induced nephropathy. After a single doxorubicin injection, survival rate of red blood cells was analyzed using 5(6)-carboxy-fluorescein-diacetate (5[6]-CFDA), SE dye, injected into the retrobulbar plexus at day 20, coinciding with development of renal failure. RBC survival was analyzed from day 20 until day 41 after induction. (**a**) Representative histograms of 5(6)-CFDA, SE fluorescence of healthy (black lines) and nephrotic mice (red lines) are shown. (**b**) Faster clearance of RBCs from the circulation in doxorubicin-injected mice compared with healthy mice. (**c**) May-Grünwald-Giemsa staining (Pappenheim method) revealed morphologic changes on day 30 in doxorubicin-injected mice (bar = 10 μm). (**d**) Ektacytometry performed on day 30 revealed that in nephrotic syndrome mice, RBC deformability was significantly affected as maximum elongation index (EI_{max}) was significantly reduced. (**e,f**) Shear stress (SS) for (**e**) $_{1/2}$ EI_{max} was significantly enhanced in doxorubicin-injected mice as well as (**f**) $SS_{1/2}$ EI_{max} ratio, indicating stiffer RBCs. Arithmetic means ± SEM are shown. *Significant difference between healthy 129S1/SvImJ and doxorubicin-injected 129S1/SvImJ mice. To optimize viewing of this image, please see the online version of this article at www.kidney-international.org.

shape. In 129S1/SvImJ mice with DIN, we observed an increased number of stomatocytes (red stars), teardrop cells (black triangle), schistocytes (black points), and microcytic cells (black arrow) (Figure 4c). *Nphs2*$^{\Delta ipod}$ mice showed an increased proportion of schistocytes (black points, Supplementary Figure S4A, lower image, left side), and cells were polychromatic (Supplementary Figure S4A, lower image, right side).

To further investigate RBC functional changes, deformability measurements on day 30 were performed using ektacytometry.[31] RBC deformability was significantly reduced in 129S1/SvImJ mice with DIN as well as in *Nphs2*$^{\Delta ipod}$ mice, as indicated by a reduced maximum elongation index (EI_{max}) (Figure 4d and Supplementary Figure S4B). Shear stress for 50% of EI_{max} (Figure 4e) and, thus, $SS_{1/2}$ EI_{max} ratio (Figure 4f) were significantly increased in 129S1/SvImJ mice with DIN, indicating stiffer RBCs. Shear stress for 50% of EI_{max} was similar in *Nphs2*$^{\Delta ipod}$ mice (Supplementary Figure S4C). $SS_{1/2}$ EI_{max} ratio tended to be augmented in *Nphs2*$^{\Delta ipod}$ mice compared with healthy C57BL/6 mice; the difference did, however, not reach statistical significance ($P = 0.06$) (Supplementary Figure S4D).

As exposure of RBCs to hypertonic extracellular conditions *in vitro* mimics the osmotic environment encountered in the

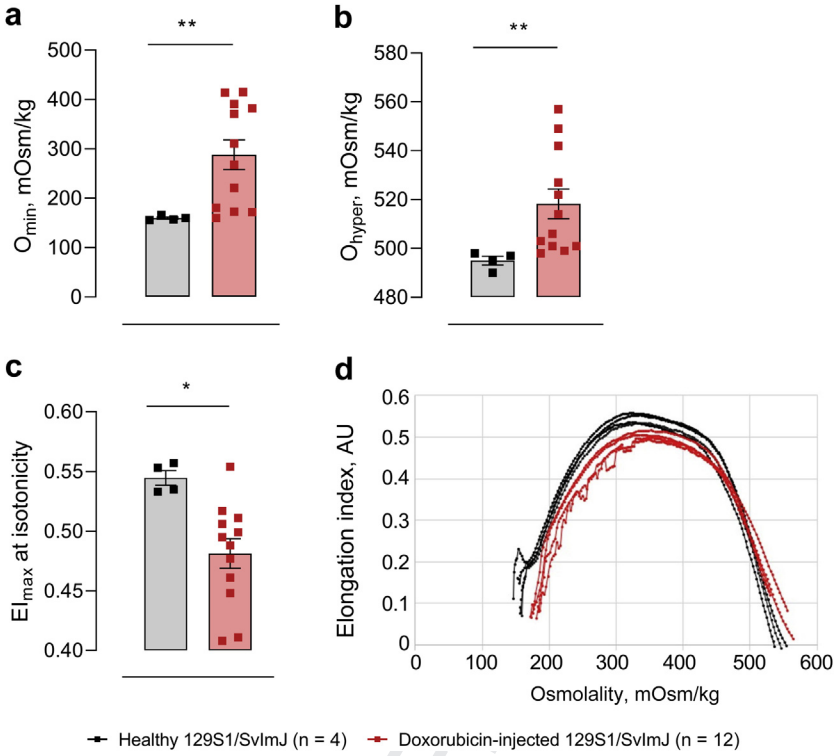

Figure 5 | Diminished osmotic resistance in doxorubicin-injected 129S1/SvImJ mice. (**a**–**c**) An osmoscan on day 30 revealed (**a**) higher O_{min} (mOsm/kg), (**b**) higher O_{hyper}, and (**c**) increased maximum elongation index (EI_{max}) at isotonicity in doxorubicin-injected 129S1/SvImJ mice. (**d**) Proportion between osmolality (mOsm/kg) and elongation index (arbitrary unit [AU]) in healthy and doxorubicin-injected 129S1/SvImJ mice, illustrating the higher elongation index of healthy mice as well as a shift in osmolality in 129S1/SvImJ mice with DIN. Arithmetic means ± SEM are shown. *Significant difference between healthy and doxorubicin-injected 129S1/SvImJ mice. **, xxx.

kidney medulla, an osmoscan was performed on day 30 and several osmosensitive parameters were determined, as described previously.[32] O_{min} represents the osmolality at minimum RBC deformability, beyond which RBCs would lyse with a further decrease in osmolarity. O_{min} values were higher in 129S1/SvImJ mice with DIN and shifted to the right (Figure 5a and d). A similar tendency toward a higher O_{min} was observed in *Nphs2*$^{\Delta ipod}$ mice (Supplementary Figure S4E). Values of O_{hyper}, reflecting the hydration state of the cells, were significantly higher in 129S1/SvImJ mice with DIN (Figure 5b), but were similar in *Nphs2*$^{\Delta ipod}$ mice and their respective control mice (Supplementary Figure S4F). The maximum deformability (EI_{max}) at isotonicity is the point at which cells have attained maximum ellipticity. EI_{max} at isotonicity was significantly reduced in 129S1/SvImJ mice with DIN (Figure 5c) but showed no differences in *Nphs2*$^{\Delta ipod}$ mice compared with healthy C57BL/6 mice (Supplementary Figure S4G). Overall, these results indicate reduced membrane integrity and elasticity but also shape changes in 129S1/SvImJ and *Nphs2*$^{\Delta ipod}$ mice as well as a higher osmotic fragility of the RBCs from 129S1/SvImJ mice with DIN.

RBCs are metabolically reprogrammed during proteinuric kidney disease in mice

To better understand the molecular adaptations associated with changes in RBC abundance and morphology as a function of kidney injury, RBCs from 129S1/SvImJ mice with DIN and *Nphs2*$^{\Delta ipod}$ mice were analyzed by mass spectrometry–based metabolomics (Figure 6a and Supplementary Figure S5A). Using this approach, the relative levels of 256 metabolites were determined for 129S1/SvImJ mice and *Nphs2*$^{\Delta ipod}$ mice. To analyze these data in a systematic manner, multivariate analyses, including partial-least squares discriminant analysis and hierarchical clustering analysis, were performed. Interestingly, partial-least squares discriminant analysis of RBC metabolomes from both models revealed similar clustering patterns. Specifically, although the samples at the time of model induction clustered together with healthy samples from all time points, samples from nephrotic mice clustered independently from healthy control samples along component 1 (Figure 6b and Supplementary Figure S5B). In line with clustering patterns evident in the 2 models, hierarchical clustering analysis of the metabolomics data for each model highlighted similar trends for metabolites involved in oxidative stress management, as well as nucleotides, amino acids, acylcarnitines, and fatty acids (Figure 6c and Supplementary Figures S5C, S6, and S7). For example, the levels of allantoin, a purine catabolite and marker of oxidative stress in RBCs,[33] and reduced glutathione both significantly accumulated over time in both nephrotic mouse models, indicating ongoing reactive oxygen species generation and activation of the antioxidant glutathione system

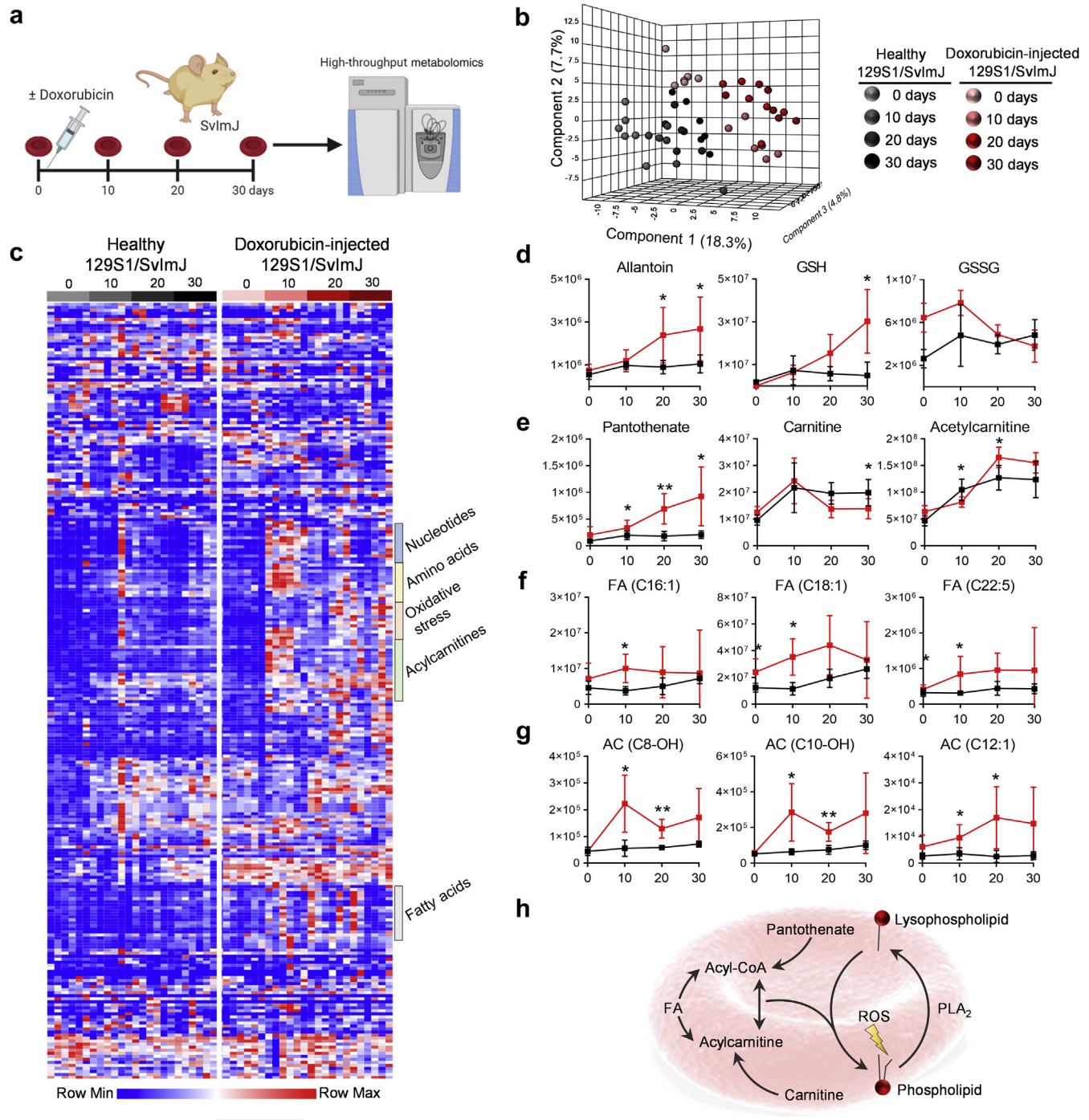

Figure 6| Metabolomics indicates accumulation of oxidative stress and activation of membrane lipid remodeling within red blood cells (RBCs) in doxorubicin-induced nephropathy. RBCs were isolated from 129S1/SvImJ control mice or those receiving a single doxorubicin injection at day 0. (**a**) Samples were extracted and analyzed by mass spectrometry–based metabolomics analysis. (**b**) Partial-least squares discriminant analysis of red blood cell samples from healthy 129S1/SvImJ mice before injection (day 0) and at 10, 20, and 30 days after injection (healthy 129S1/SvImJ mice samples colored from gray to black during time progression, and doxorubicin-injected samples colored from pink to red during time progression). Hierarchical clustering analysis of metabolomics data. Values are colored from blue to red according to Z-score normalized values from row minimum to maximum, respectively. (**c**) Areas enriched with compounds from oxidative stress, amino acid, nucleotide, acylcarnitine, and fatty acid (FA) compound classes are indicated. (**d**) Relative levels of oxidative stress metabolites allantoin, reduced glutathione (GSH), and oxidized glutathione (GSSG) in RBCs over time are shown for healthy 129S1/SvImJ (black) or doxorubicin-injected 129S1/SvImJ mice (red). (**e**) Relative levels of coenzyme A (CoA) precursor pantothenate, carnitine, and acetyl carnitine are shown. (**f**) Relative levels of FAs hexadecenoic acid (C16:1), octadecenoic acid (C18:1), and docosapentaenoic acid (C22:5) are shown. (**g**) Relative levels of hydroxyoctanoyl-carnitine (AC C8-OH), hydroxydecanoyl-carnitine (AC C10-OH), and dodecanoyl-carnitine (AC C12:1) are displayed. (**h**) A pathway overview of RBC membrane lipid remodeling. All *y*-axes values are given in arbitrary units. *Significant difference between healthy 129S1/SvImJ and doxorubicin-injected 129S1/SvImJ mice. PLA_2, xxx; ROS, reactive oxygen species.

(Figure 6d and Supplementary Figure S5D). Likewise, the levels of the coenzyme A (CoA) precursor pantothenate accumulated over time (Figure 6e and Supplementary Figure S5E).

Similar patterns were evident in the levels of the free fatty acids hexadecenoic acid (C16:1), octadecenoic acid (C18:1), and docosapentaenoic acid (C22:5), although each model had unique temporal patterns (Figure 6f and Supplementary Figure S5F).

On top of fatty acids, acylcarnitines, including hydroxyoctanoyl-carnitine (AC C8-OH), hydroxydecanoyl-carnitine (AC C10-OH), and dodecanoyl-carnitine (AC C12:1), also responded to induction of proteinuric nephropathy in both models (Figure 6g and Supplementary Figure S5G).

Taken together, these findings suggest that on induction of proteinuric kidney disease in 2 similar mouse models, increased levels of oxidative stress may impart damage to acyl chains on membrane lipids. Because RBCs are devoid of the capacity to synthesize new lipids, they make use of a system that depends on phospholipase-mediated removal of damaged acyl chains and replacement with undamaged fatty acids. Referred to as the Lands cycle,[34] this system depends on acyl-chain activation by conjugation to CoA, which establishes an equilibrium with acyl carnitine for membrane replacement[35] (Figure 6h and Supplementary Figure S5H).

Proteinuric CKD patients with anemia display enhanced RBC death

To confirm that PS-exposing RBCs occur also in human CKD, as described earlier,[36] we analyzed blood samples from 25 patients treated by our outpatient clinic. To match the mouse models that represent nephrotic syndrome with preserved GFR during the first 10 days, and then advanced CKD with reduced GFR from day 20 onwards (Figure 1 and Supplementary Figure S2), we analyzed 10 patients with primary nephrotic syndrome representing proteinuric CKD with preserved GFR (>60 ml/min per 1.73 m^2) and 15 patients with CKD with nephrotic-range proteinuria and GFR <60 ml/min per 1.73 m^2. The patient characteristics are shown in Table 1. Renal anemia, as defined by a hemoglobin concentration <13.5 g/dl in men and <12 g/dl in women, was observed in 4 of the 10 nephrotic patients (red triangles in Figure 7), whereas 14 of 15 CKD patients with nephrotic-range proteinuria and reduced GFR were anemic (Figure 7a). In the latter group, plasma EPO concentrations and reticulocyte production index were not increased (Figure 7b and c), consistent with reduced erythropoiesis. In fluorescence-activated cell sorting analysis, nephrotic patients and patients with advanced CKD had a higher rate of PS-exposing cells (mean, 1.0% ± 0.3% and 1.4% ± 0.7%, respectively) compared with healthy subjects (mean, 0.6% ± 0.1%; Figure 7d). RBC cell death in patients with nephrotic syndrome and advanced CKD was triggered by higher levels of reactive oxygen species (Figure 7e) and increased ceramide levels (Figure 7f). Augmented intracellular calcium concentration was found in patients with advanced CKD (Figure 7g).

Human RBCs from patients with nephrotic syndrome and advanced CKD showed morphologic alterations, as observed in the mouse models (Figures 4c and 7j–l and Supplementary Figure 3A). Although RBC morphology was normal in controls, anemic patients with nephrotic syndrome and advanced CKD patients had an increased number of teardrop cells (black triangles) and echinocytes (black crosses) (Figure 7k and l). In addition, target cells occurred in nephrotic patients with anemia and in patients with advanced CKD (red crosses; Figure 7k and l). All patient groups, including nephrotic patients without anemia, had an increased proportion of spherocytes (blue arrows; Figure 7j–l).

To analyze deformability of human RBCs, ektacytometry was performed. In comparison to healthy controls, maximum deformability (EI_{max}) was reduced in patients with advanced CKD (Figure 7h); EI_{max} tended to be lower in patients with primary nephrotic syndrome without reaching statistical significance (Figure 7h). The parameters $SS_{1/2}$, O_{min}, O_{hyper}, and EI_{max} at isotonicity were not significantly different between healthy controls, nephrotic patients, and patients with advanced CKD (Supplementary Figure S8A–D).

DISCUSSION

The present study reveals novel pathophysiological mechanisms leading to renal anemia in 2 murine models of proteinuric kidney disease with severely impaired renal function. Our study demonstrates that in these models, anemia is the result of a reduced RBC lifespan triggered by exposure of PS and accelerated phagocytic clearance. Intriguingly, anemia in these mice developed despite stimulated erythropoiesis, suggesting that reduced RBC lifespan, through increased RBC cell death, might be an alternative explanation for these findings. Contrary to CKD patients with anemia (Figure 7,[7]), both Q11 mouse models were characterized by increased plasma EPO concentration. This can be surmised by preservation of EPO-secreting ability in these models that probably spares the EPO-secreting cells located in the renal interstitium. The increased EPO secretion in these models, however, does not invalidate the conclusion that RBC cell death is a major player in the pathogenesis of renal anemia. On the contrary, stimulation of erythropoiesis by increased EPO secretion can be considered as a compensatory mechanism to increased RBC death induced by renal failure in these models. Along the lines, increased extramedullary erythropoiesis with increased spleen volume was recently observed in another proteinuric mouse model with anemia.[37]

In patients with proteinuric CKD and concomitant anemia, we also observed an increased percentage of PS-exposing RBCs along with higher levels of reactive oxygen species and ceramide. This suggests that accelerated RBC death might be involved in the pathogenesis of renal anemia in human CKD. Plasma EPO concentrations and reticulocyte production index were not increased in anemic CKD patients, pointing to reduced erythropoiesis, which in concert with RBC death is expected to aggravate renal anemia. The reasons for the loss of renal EPO secretion in human CKD remain unclear.

FLA 5.6.0 DTD ■ KINT2759_proof ■ 7 October 2021 ■ 12:12 am ■ ce

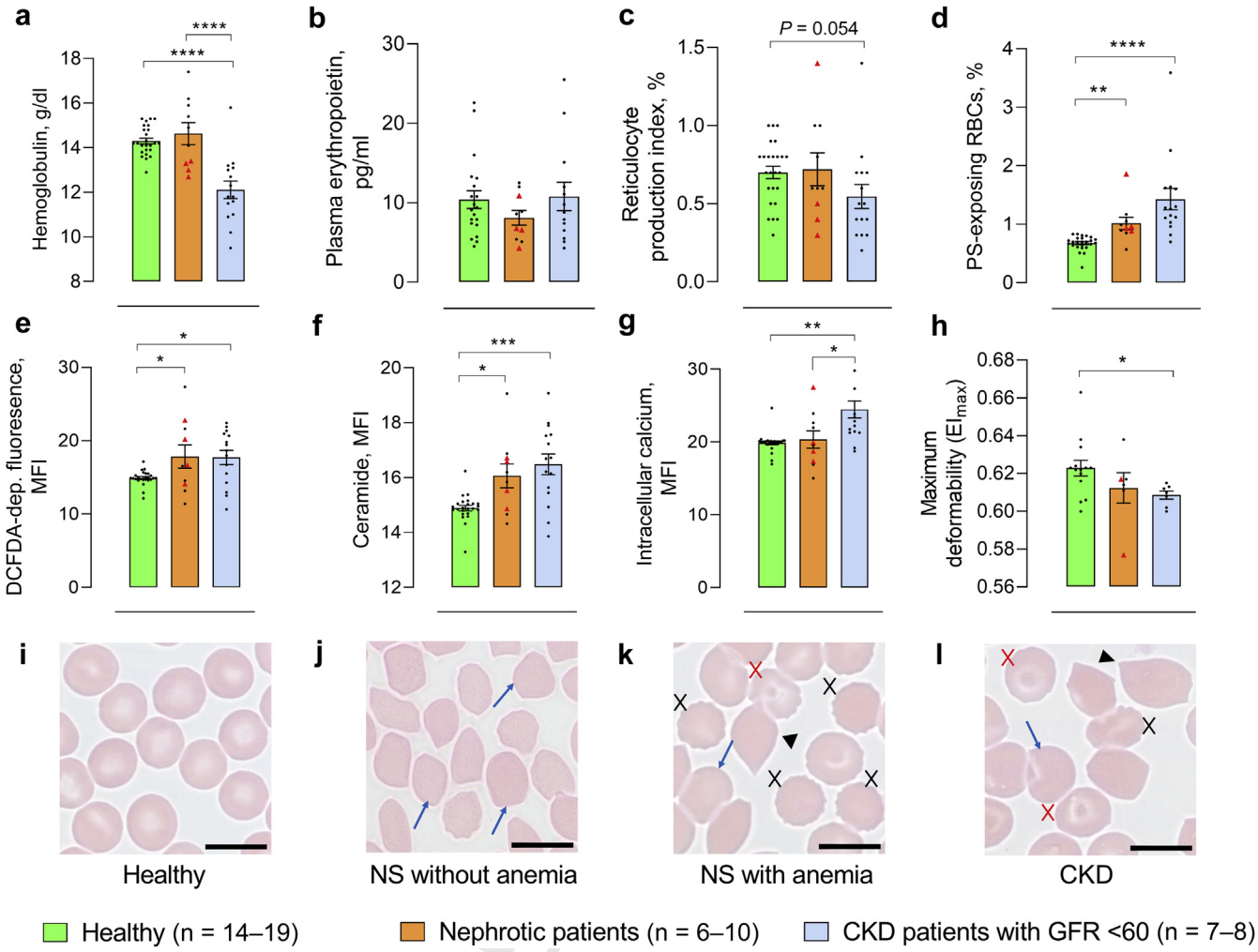

Figure 7 | Red blood cell (RBC) death in proteinuric chronic kidney disease (CKD) patients with anemia. (**a–c**) The (**a**) hemoglobin, (**b**) plasma erythropoietin concentration, and (**c**) reticulocyte production index in healthy, nephrotic patients and patients with advanced CKD. (**d–f**) Percentages of (**d**) phosphatidylserine (PS)–exposing RBCs, (**e**) DCFDA fluorescence, and (**f**) ceramide-dependent fluorescence as factors Q27 associated with RBC death were augmented in nephrotic patients and in patients with advanced CKD. (**g**) Intracellular calcium concentration was enhanced in advanced CKD patients. (**h**) Ektacytometry measurements revealed that RBC deformability of patients with advanced CKD was significantly impaired, as indicated by a diminished maximum elongation index (EI_{max}). (**i–l**) May-Grünwald-Giemsa staining (Pappenheim method) revealed morphologic alterations in nephrotic syndrome patients (**j**) without anemia and (**k**) with anemia, and in (**l**) patients with advanced CKD compared with RBCs obtained from (**i**) healthy donors. Arithmetic means ± SEM are shown. *Significant difference between Q28 groups. Dep., dependent. To optimize viewing of this image, please see the online version of this article at www.kidney-international.org. GFR, glomerular filtration rate; MFI, mean fluorescence intensity; NS, not significant.

Remarkably, although not all patients with normal GFR had anemia, those with reduced GFR were all anemic, pointing to an effect of long-standing and advanced CKD. Notably, the relative EPO deficit in CKD can be overcome by using the new class of prolyl hydroxylase inhibitors,[38] suggesting perturbed oxygen sensing as a possible cause for EPO hyposecretion.

Our data demonstrate diminished RBC deformability in both mouse models of proteinuric nephropathy, which may be directly related to elevated cytoplasmic Ca^{2+} levels.[39] Together, these mechanisms could act in concert to facilitate the induction of RBC cell death and removal of senescent and injured RBCs from the blood circulation.[15] Furthermore, we observed metabolic reprogramming in these cells, indicative of oxidative stress and membrane lipid remodeling. Although CoA and acyl-CoA were not directly measured in these samples, they are actively converted in RBCs to acylcarnitines by carnitine palmitoyl transferase.[35] Accumulating levels of the latter compound class indicate activation of these mechanisms in nephropathy, as these metabolites are not readily transported across RBC membranes.[40] In further support, we observed accumulation in both models of CoA precursors, including pantothenate, which is taken up[41] and metabolized[42] by RBCs, in parallel to increasing free fatty acids and decreasing free carnitine. Interestingly, we previously found that these alterations occur in association with supraphysiologic levels of intracellular Ca^{2+}.[16] Although those results were generated *ex vivo*, we report herein similar

responses *in vivo*. Furthermore, acylcarnitines are capable of directly modulating membrane properties[43] and correlate with RBC deformability,[44] as well as osmotic and oxidative hemolysis.[45] Unconjugated free carnitine promotes membrane deformability through the mediation of interactions between membrane proteins.[46] Our observations of significantly decreased levels of carnitine in RBCs from mice with nephropathy, presumably due to increased consumption for the generation of acylcarnitines, may contribute to the impaired rheological parameters we observed in parallel.

Our findings suggest common mechanisms leading to RBC death in mice with both DIN and podocin deficiency, which may be related to both nephrotic-range proteinuria and, more important, development of severe renal failure in the mouse models observed from day 20 on. In humans, advanced CKD with reduced GFR is a strong predictor of anemia,[47] and stimulation of RBC death could be related to the uremic milieu. One has to acknowledge that in advanced CKD, many factors and derangements might come into play and promote renal anemia. The contribution of heavy proteinuria to the stimulation of RBC death remains unclear, but, although not proven, might involve factors that are lost in the urine, such as transferrin or others regulating RBC metabolism.[48] So far, current treatment of renal anemia focuses on increasing erythropoiesis by iron or EPO substitution,[49] by application of oral hypoxia-inducible factor protein stabilizers,[50] or by oral or i.v. iron administration.[51] However, these treatments do not consider increased RBC death. In a previous cross-sectional study in hemodialysis and peritoneal dialysis patients, we found that patients with a higher percentage of PS-exposing RBCs were treated with higher EPO doses.[14] Therefore, amelioration of RBC cell death promises to be a possible therapeutic approach in treating renal anemia. In this context, the inhibitory effect of various pharmacologic agents on RBC cell death[52] requires further human and animal studies.

In conclusion, altered cellular metabolism contributes to RBC dysfunction, enhanced RBC death, and hence anemia in mouse models of proteinuric CKD, despite increased serum EPO levels. The findings of this study may partly explain the mechanisms of anemia associated with CKD in humans.

DISCLOSURE

Q12 Although unrelated to the contents of the articles, AD and TN are founders of Omix Technologies, Inc. All the other authors declared no competing interests.

DATA STATEMENT

Data will be made available on reasonable request.

ACKNOWLEDGEMENTS

The authors acknowledge the expert technical assistance of Andrea Janessa. These studies were supported by a grant from the German Research Foundation to RB (BI 2149/2-1) and FA (AR 1092/2-2). LS was Q13 supported by an IZKF grant by the medical faculty of Tübingen Q33 University. SMQ was supported by resources from Canadian Blood Services. As a condition of Canadian government funding, this report must contain the statement "The view expressed herein do not necessarily represent the view of the federal government of Canada."

AUTHOR CONTRIBUTIONS

RB and FA designed the study. Data collection was performed by RB, TN, MG, TD, DE, MW, LS, MX, JMB, MZK, KO, LK, IG-M, and BF. Q14 Statistical analyses were conducted by RB, TN, MG, TD, LS, JMB, LK, IG-M, and AD; and figures were generated by RB, TN, MZK, IG-M, LQ-M, Q15 BF, and AD. RB, TN, AD, MG, BNB, LS, AS, TB, MS, ALB, FG, SMQ, and FA interpreted the data. The manuscript was written, reviewed, and edited by RB, TN, AD, MG, BNB, TB, ALB, FG, SMQ, and FA.

SUPPLEMENTARY MATERIAL

Supplementary File (PDF)

Figure S1. Experimental design of the studies in 129S1/SvImJ and *Nphs2*$^{\Delta ipod}$ mice.

Figure S2. Deletion of podocin expression and hallmarks of nephrotic syndrome in *Nphs2*$^{\Delta ipod}$ mice.

Figure S3. Reduced red blood cell survival rate in experimental nephrotic syndrome in *Nphs2*$^{\Delta ipod}$ mice.

Figure S4. Altered morphology and reduced deformability of red blood cells in *Nphs2*$^{\Delta ipod}$ mice.

Figure S5. Metabolomics indicates accumulation of oxidative stress and activation of membrane lipid remodeling within red blood cells in *Nphs2*$^{\Delta ipod}$ mice.

Figure S6. Metabolomics indicates altered metabolism within red blood cells obtained from 129S1/SvImJ mice.

Figure S7. Metabolomics indicates altered metabolism within red blood cells received from *Nphs2*$^{\Delta ipod}$ mice.

Figure S8. Shear stress at one-half of maximum red blood cell (RBC) deformability and RBC osmotic sensitivity are not significantly different in primary nephrotic syndrome and advanced patients with chronic kidney disease (CKD).

REFERENCES

1. Finkelstein FO, Story K, Firanek C, et al. Health-related quality of life and hemoglobin levels in chronic kidney disease patients. *Clin J Am Soc Nephrol*. 2009;4:33–38.
2. Efstratiadis G, Konstantinou D, Chytas I, et al. Cardio-renal anemia syndrome. *Hippokratia*. 2008;12:11–16.
3. Staples AO, Wong CS, Smith JM, et al. Anemia and risk of hospitalization in pediatric chronic kidney disease. *Clin J Am Soc Nephrol*. 2009;4:48–56.
4. Kurella Tamura M, Vittinghoff E, Yang J, et al. Anemia and risk for cognitive decline in chronic kidney disease. *BMC Nephrol*. 2016;17:13.
5. Toft G, Heide-Jørgensen U, van Haalen H, et al. Anemia and clinical outcomes in patients with non-dialysis dependent or dialysis dependent severe chronic kidney disease: a Danish population-based study. *J Nephrol*. 2020;33:147–156.
6. Geddes CC. Pathophysiology of renal anaemia. *Nephrol Dial Transplant*. 2018;34:921–922.
7. Artunc F, Risler T. Serum erythropoietin concentrations and responses to anaemia in patients with or without chronic kidney disease. *Nephrol Dial Transplant*. 2007;22:2900–2908.
8. Erslev AJ, Besarab A. Erythropoietin in the pathogenesis and treatment of the anemia of chronic renal failure. *Kidney Int*. 1997;51:622–630.
9. Wish JB, Aronoff GR, Bacon BR, et al. Positive iron balance in chronic kidney disease: how much is too much and how to tell? *Am J Nephrol*. 2018;47:72–83.
10. Howard RL, Buddington B, Alfrey AC. Urinary albumin, transferrin and iron excretion in diabetic patients. *Kidney Int*. 1991;40:923–926.
11. Joske RA, McAlister JM, Prankerd TA. Isotope investigations of red cell production and destruction in chronic renal disease. *Clin Sci*. 1956;15:511–522.
12. Loge JP, Lange RD, Moore CV. Characterization of the anemia associated with chronic renal insufficiency. *Am J Med*. 1958;24:4–18.
13. Li JH, Luo JF, Jiang Y, et al. Red blood cell lifespan shortening in patients with early-stage chronic kidney disease. *Kidney Blood Press Res*. 2019;44:1158–1165.

14. Bissinger R, Artunc F, Qadri SM, et al. Reduced erythrocyte survival in uremic patients under hemodialysis or peritoneal dialysis. *Kidney Blood Press Res*. 2016;41:966–977.
15. Qadri SM, Bissinger R, Solh Z, et al. Eryptosis in health and disease: a paradigm shift towards understanding the (patho)physiological implications of programmed cell death of erythrocytes. *Blood Rev*. 2017;31:349–361.
16. Nemkov T, Qadri SM, Sheffield WP, et al. Decoding the metabolic landscape of pathophysiological stress-induced cell death in anucleate red blood cells. *Blood Transfus*. 2020;18:130–142.
17. Larsson A, Hult A, Nilsson A, et al. Red blood cells with elevated cytoplasmic Ca2+ are primarily taken up by splenic marginal zone macrophages and CD207+ dendritic cells. *Transfusion*. 2016;56:1834–1844.
18. Bohnert BN, Menacher M, Janessa A, et al. Aprotinin prevents proteolytic epithelial sodium channel (ENaC) activation and volume retention in nephrotic syndrome. *Kidney Int*. 2018;93:159–172.
19. Xiao M, Bohnert BN, Aypek H, et al. Plasminogen deficiency does not prevent sodium retention in a genetic mouse model of experimental nephrotic syndrome. *Acta Physiol (Oxf)*. 2021;231:e13512.
20. Artunc F, Nasir O, Amann K, et al. Serum- and glucocorticoid-inducible kinase 1 in doxorubicin-induced nephrotic syndrome. *Am J Physiol Renal Physiol*. 2008;295:F1624–F1634.
21. Bohnert BN, Daniel C, Amann K, et al. Impact of phosphorus restriction and vitamin D-substitution on secondary hyperparathyroidism in a proteinuric mouse model. *Kidney Blood Press Res*. 2015;40:153–165.
22. Zheng Z, Schmidt-Ott KM, Chua S, et al. A Mendelian locus on chromosome 16 determines susceptibility to doxorubicin nephropathy in the mouse. *Proc Natl Acad Sci U S A*. 2005;102:2502–2507.
23. Becker HM, Chen M, Hay JB, et al. Tracking of leukocyte recruitment into tissues of mice by *in situ* labeling of blood cells with the fluorescent dye CFDA SE. *J Immunol Methods*. 2004;286:69–78.
24. Baskurt OK, Hardeman MR, Uyuklu M, et al. Comparison of three commercially available ektacytometers with different shearing geometries. *Biorheology*. 2009;46:251–264.
25. Da Costa L, Suner L, Galimand J, et al. Diagnostic tool for red blood cell membrane disorders: assessment of a new generation ektacytometer. *Blood Cells Mol Dis*. 2016;56:9–22.
26. Bissinger R, Lang E, Ghashghaeinia M, et al. Blunted apoptosis of erythrocytes in mice deficient in the heterotrimeric G-protein subunit Gαi2. *Sci Rep*. 2016;6:30925.
27. Nemkov T, Reisz JA, Gehrke S, et al. High-throughput metabolomics: isocratic and gradient mass spectrometry-based methods. In: D'Alessandro A, ed. *High-Throughput Metabolomics: Methods and Protocols*. New York, NY: Springer New York; 2019:13–26.
28. Nasr SH, Markowitz GS, Reddy BS, et al. Dysproteinemia, proteinuria, and glomerulonephritis. *Kidney Int*. 2006;69:772–775.
29. Kaestner L, Bogdanova A, Egee S. Calcium channels and calcium-regulated channels in human red blood cells. *Adv Exp Med Biol*. 2020;1131:625–648.
30. Huber SM, Duranton C, Lang F. Patch-clamp analysis of the "new permeability pathways" in malaria-infected erythrocytes. *Int Rev Cytol*. 2005;246:59–134.
31. Nemeth N, Kiss F, Miszti-Blasius K. Interpretation of osmotic gradient ektacytometry (osmoscan) data: a comparative study for methodological standards. *Scand J Clin Lab Invest*. 2015;75:213–222.
32. Zaidi AU, Buck S, Gadgeel M, et al. Clinical diagnosis of red cell membrane disorders: comparison of osmotic gradient ektacytometry and eosin maleimide (EMA) fluorescence test for red cell band 3 (AE1, SLC4A1) content for clinical diagnosis. *Front Physiol*. 2020;11:636.
33. Kand'ár R, Záková P. Allantoin as a marker of oxidative stress in human erythrocytes. *Clin Chem Lab Med*. 2008;46:1270–1274.
34. Lands WE. Metabolism of glycerolipides; a comparison of lecithin and triglyceride synthesis. *J Biol Chem*. 1958;231:883–888.
35. Arduini A, Mancinelli G, Radatti GL, et al. Role of carnitine and carnitine palmitoyltransferase as integral components of the pathway for membrane phospholipid fatty acid turnover in intact human erythrocytes. *J Biol Chem*. 1992;267:12673–12681.
36. Bonomini M, Sirolli V, Settefrati N, et al. Increased erythrocyte phosphatidylserine exposure in chronic renal failure. *J Am Soc Nephrol*. 1999;10:1982–1990.
37. Maier JI, Rogg M, Helmstädter M, et al. A novel model for nephrotic syndrome reveals associated dysbiosis of the gut microbiome and extramedullary hematopoiesis. *Cells*. 2021;10:1509.
38. Schödel J, Ratcliffe PJ. Mechanisms of hypoxia signalling: new implications for nephrology. *Nat Rev Nephrol*. 2019;15:641–659.
39. Barodka V, Mohanty JG, Mustafa AK, et al. Nitroprusside inhibits calcium-induced impairment of red blood cell deformability. *Transfusion*. 2014;54:434–444.
40. Cooper MB, Forte CA, Jones DA. Carnitine and acetylcarnitine in red blood cells. *Biochim Biophys Acta*. 1988;959:100–105.
41. Annous KF, Song WO. Pantothenic acid uptake and metabolism by red blood cells of rats. *J Nutr*. 1995;125:2586–2593.
42. Brohn FH, Trager W. Coenzyme A requirement of malaria parasites: enzymes of coenzyme A biosynthesis in normal duck erythrocytes and erythrocytes infected with *Plasmodium lophurae*. *Proc Natl Acad Sci U S A*. 1975;72:2456–2458.
43. Arduini A, Rossi M, Mancinelli G, et al. Effect of L-carnitine and acetyl-L-carnitine on the human erythrocyte membrane stability and deformability. *Life Sci*. 1990;47:2395–2400.
44. Nemkov T, Skinner SC, Nader E, et al. Acute cycling exercise induces changes in red blood cell deformability and membrane lipid remodeling. *Int J Mol Sci*. 2021;22:896.
45. Alexander K, Hazegh K, Fang F, et al. Testosterone replacement therapy in blood donors modulates erythrocyte metabolism and susceptibility to hemolysis in cold storage. *Transfusion*. 2021;61:108–123.
46. Butterfield DA, Rangachari A. Acetylcarnitine increases membrane cytoskeletal protein-protein interactions. *Life Sci*. 1993;52:297–303.
47. Stauffer ME, Fan T. Prevalence of anemia in chronic kidney disease in the United States. *PLoS One*. 2014;9:e84943.
48. Prinsen B, Velden M, Kaysen GA, et al. Transferrin synthesis is increased in nephrotic patients insufficiently to replace urinary losses. *J Am Soc Nephrol*. 2001;12:1017–1025.
49. Agoro R, Montagna A, Goetz R, et al. Inhibition of fibroblast growth factor 23 (FGF23) signaling rescues renal anemia. *FASEB J*. 2018;32:3752–3764.
50. Beck H, Jeske M, Thede K, et al. Discovery of molidustat (BAY 85-3934): a small-molecule oral HIF-prolyl hydroxylase (HIF-PH) inhibitor for the treatment of renal anemia. *ChemMedChem*. 2018;13:988–1003.
51. Macdougall IC, Bircher AJ, Eckardt KU, et al. Iron management in chronic kidney disease: conclusions from a "Kidney Disease: Improving Global Outcomes" (KDIGO) Controversies Conference. *Kidney Int*. 2016;89:28–39.
52. Pretorius E, du Plooy JN, Bester J. A comprehensive review on eryptosis. *Cell Physiol Biochem*. 2016;39:1977–2000.